



Theoretical Considerations and a Mathematical Model for the Analysis of the Biomechanical Response of Human Keratinized Oral Mucosa

Aikaterini Tsaira¹, Panagiotis Karagiannidis^{2,3}, Margarita Sidira¹, Spyros Kassavetis², Dimitris Kugiumtzis⁴, Stergios Logothetidis², Olga Naka¹, Argirios Pissiotis¹ and Konstantinos Michalakis^{1,5*}

¹ Department of Prosthodontics, Faculty of Health Sciences, School of Dentistry, Aristotle University, Thessaloniki, Greece,

² Laboratory of Thin Films-Nanosystems and Nanometrology, School of Physics, Aristotle University, Thessaloniki, Greece,

³ Department of Engineering, Cambridge Graphene Centre, Cambridge University, Cambridge, UK, ⁴ Department of Electrical and Computer Engineering, School of Engineering, Aristotle University, Thessaloniki, Greece, ⁵ Division of Graduate and Postgraduate Prosthodontics, Tufts University School of Dental Medicine, Boston, MA, USA

OPEN ACCESS

Edited by:

Thimios Mitsiadis,
University of Zurich, Switzerland

Reviewed by:

Jean-Christophe Farges,
Claude Bernard University Lyon 1,
France

Christian Hellmich,
Vienna University of Technology,
Austria

Nenad Filipovic,
University of Kragujevac, Serbia

*Correspondence:

Konstantinos Michalakis
kmichalakis@hotmail.com;
konstantinos.michalakis@tufts.edu;
kmichalakis@dent.auth.gr

Specialty section:

This article was submitted to
Craniofacial Biology,
a section of the journal
Frontiers in Physiology

Received: 28 May 2016

Accepted: 09 August 2016

Published: 29 August 2016

Citation:

Tsaira A, Karagiannidis P, Sidira M, Kassavetis S, Kugiumtzis D, Logothetidis S, Naka O, Pissiotis A and Michalakis K (2016) Theoretical Considerations and a Mathematical Model for the Analysis of the Biomechanical Response of Human Keratinized Oral Mucosa. *Front. Physiol.* 7:364. doi: 10.3389/fphys.2016.00364

Removable complete and partial dentures are supported by the residual alveolar ridges consisting of mucosa, submucosa, periosteum, and bone. An understanding of the biomechanical behavior of the oral mucosa is essential in order to improve the denture-bearing foundations for complete and partially edentulous patients. The purpose of this paper was to examine the biomechanical behavior of the soft tissues supporting a removable denture and develop a model for that reason. Keratinized oral mucosa blocks with their underlying bone were harvested from the maxillary palatal area adjacent to the edentulous ridges of a cadaver. The compressive response of the oral mucosa was tested by using atomic force microscopy. The specimens were first scanned in order their topography to be obtained. The mechanical properties of the specimens were tested using a single crystal silicon pyramidal tip, which traversed toward the keratinized oral mucosa specimens. Loading-unloading cycles were registered and four mathematical models were tested using MATLAB to note which one approximates the force-displacement curve as close as possible: a. spherical, b. conical, c. third order polynomial, d. Murphy (fourth order polynomial, non-linear Hertzian based). The third order polynomial model showed the best accuracy in representing the force-displacement data of the tested specimens. A model was developed in order to analyze the biomechanical behavior of the human oral keratinized mucosa and obtain information about its mechanical properties.

Keywords: human oral keratinized mucosa, atomic force microscopy, oral tissue mechanics, contact mechanics, polynomial model, mathematical model, curve fitting

INTRODUCTION

Removable complete and partial dentures are supported by the residual alveolar ridges consisting of mucosa, submucosa, periosteum, and bone. This supporting area has been calculated to be 23 cm² for the maxilla, and about 12.25 cm² for the edentulous mandible (Hobkirk and Zarb, 2013). It should be mentioned however that these figures vary, depending on the size of the

maxilla or mandible and the amount of resorption after teeth extraction. Nevertheless, these numbers are substantially lower than the supporting mechanism of the teeth—i.e., the periodontal ligament—which is about 45 cm², for each dental arch (Hobkirk and Zarb, 2013).

Besides the smaller area of the denture bearing surface in comparison with that of the teeth, there are some other distinct differences too. These include the involved sensory mechanisms and the anatomical features of each structure. The periodontal ligament is connective tissue with a thickness of 0.15–0.35 mm, consisting of collagen, oxytalan and eulanin fibers, glycosaminoglycans and blood vessels ranging between 4 and 47% of the total tissue volume (Jonas and Riede, 1980; Blaushild et al., 1992; Johnson and Pylypas, 1992; Embery et al., 1995; Sloan and Carter, 1995; Michalakis et al., 2012). The periodontal ligament is organized into six different groups of fibers which are not unidirectionally distributed: 1. transeptal, 2. alveolar crest, 3. horizontal, 4. oblique, 5. apical, and 6. interradicular, which are present only between the roots of multirrooted teeth (Carranza, 1990; Lindhe et al., 2003). The existence of many blood vessels into the periodontal ligament and the hemodynamic pressure that these vessels exert affects its biomechanical response (Kristiansen and Heyreass, 1989; Sims, 1995; Ioi et al., 2002a,b). The biomechanical response of the periodontal ligament to occlusal loads is not clear (Caputo and Standlee, 1987). Three focal hypotheses have been made in the past, in order to describe the way in which the periodontal ligament supports the tooth: (i) the tensional mechanism model, supporting the idea that the fibers have a wavy configuration and consequently load transmission from the tooth to the neighboring alveolar bone occurs through a gradual unfolding of these fibers (Mühlemann, 1951; Picton, 1965, 1969), (ii) the viscoelastic model, considering that tooth movement within the socket is controlled more by the vascular elements than by the fibers (Bien, 1966; Fung, 1973; Natali et al., 2004), (iii) the collagenous thixotropic model, supporting the notion that tooth support is possible because of the periodontal ligament's thixotropic gel properties (Kardos and Simpson, 1979, 1980).

The oral mucosa covering the hard palate and the attached gingiva is termed masticatory mucosa and consists of the stratified squamous epithelium at the surface and the lamina propria which lies deeper. The stratified squamous epithelium consists of four layers, which—from most superficial to deepest—are: (a) stratum corneum, (b) stratum granulosum, (c) stratum spinosum, (d) stratum basale (Nanci, 2013). Lamina propria is connective tissue, which is composed of cells, mainly fibroblasts, and an extracellular matrix, consisting of a ground substance and fibers. Fibroblasts are responsible for the secretion of collagen and other elements of the extracellular matrix. The ground substance of the matrix is composed of glycoproteins, glycosaminoglycans and proteoglycans, while the fibers are mainly collagen, providing tensile strength and flexibility to the tissue and elastic fibers, contributing resiliency. Below the oral mucosa of the attached gingiva and the hard palate lies the mucoperiosteum with dense collagenous connective tissue attaching directly to the periosteum. The mucoperiosteum contains fat and salivary glands (Slavkin and Bavetta, 1972;

Newcomb, 1981; Clausen et al., 1983; Meyer et al., 1984; Dahllöf et al., 1986; Bourke et al., 2000). An understanding of the biomechanical behavior of the oral mucosa is essential in order to improve the denture-bearing foundations for complete and partially edentulous patients, by better managing traumatized tissues and giving instructions to patients regarding the time which is required for tissues to recover, after applying occlusal loads during daytime. Furthermore, finite element analysis models studying the deformation of oral mucosa under occlusal loading require use of an equation, which unfortunately is not supplied by the bibliography. Nevertheless, finite element analyses of the oral mucosa have been performed in the past and several material models have been adopted in order mucosal behavior to be interpreted. These include linear elastic, biphasic, multi-phasic elastic, and hyperelastic models (Chen et al., 2015). Additionally, knowledge of oral mucosa biomechanics can be helpful in fabricating dental materials with similar or complementary behavior to that of oral tissues (Saitoh et al., 2010; Hong et al., 2012).

Although, numerous articles have been published on the biomechanics of the periodontal ligament (Kurashima, 1965; Komatsu and Viidik, 1966; Daly et al., 1974; Wills et al., 1976; Atkinson and Ralph, 1977; Wills and Picton, 1978; Dorow et al., 2003; Natali et al., 2003; Bergomi et al., 2010, 2011), the research on the biomechanics of keratinized oral mucosa is scarce (Keilig et al., 2009; Goktas et al., 2011).

The purpose of this study was to examine the biomechanical behavior of the soft tissues supporting a removable complete denture and develop a model for that reason.

MATERIALS AND METHODS

Tissue Preparation

This *in vitro* study was performed in accordance with the guidelines of the Declaration of Helsinki and the research protocol was approved by the Ethics Committee of the Aristotle University (256/06-07-2011), prior to initiation.

Eight 12 × 8 × 8 mm keratinized oral mucosa blocks with their underlying bone were provided by the Laboratory of Anatomy of the Medical Faculty of the Health Sciences School of the Aristotle University of Thessaloniki (Goktas et al., 2011; Herris et al., 2013). The specimens were harvested from maxillary edentulous areas, by using a low speed 0.2 mm thickness diamond disc (Thin Flex X929-7 TP; Abrasive Technology Inc, Lewis Center, OH, USA) under continuous saline irrigation (**Figure 1**). To prevent dehydration, the specimens were then stored in a 10% neutral buffered formalin solution (water 91.9–92%, formaldehyde 4%, methyl alcohol 1–2%, sodium phosphate dibasic 0.65%, sodium phosphate monobasic, monohydrate 0.4%) until the mechanical analysis testing, which took place 1 h after.

The compressive response of the oral mucosa was the only biomechanical characteristic tested, by using an Atomic Force Microscope (Solver P47H; NT-MDT Co., Moscow, Russia). A standard square based pyramidal single crystal silicon (Si) tip (NSG 10; NT-MDT Co., Moscow, Russia) with a <10 nm typical curvature tip radius and a lateral surface of 500 μm was used. A nominal spring constant of 12.9 0.06 N/m was used after



FIGURE 1 | Human keratinized oral mucosa specimen with the underlying bone, tested with AFM.

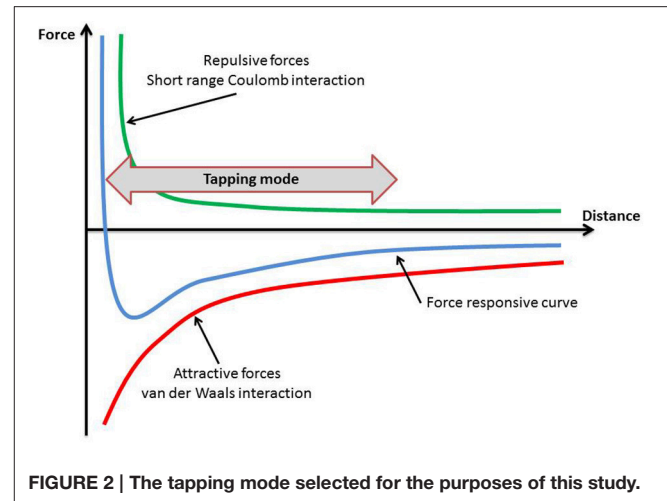


FIGURE 2 | The tapping mode selected for the purposes of this study.

calculating it by using the Sader method (Sader et al., 1999). The length of the cantilever was $95 \pm 5 \mu\text{m}$, the width was $30 \pm 3 \mu\text{m}$, while the thickness was $2 \pm 0.5 \mu\text{m}$.

Before initiation of the experimental procedures a calibration of the cantilever took place. First the deflection was converted to force using the Hooke's law and then the response of the cantilever was subtracted from the measurement. For this purpose a force-displacement curve in a hard surface was acquired, followed by a force-displacement curve on the sample. The difference of these measurements supplied the indentation depth.

The specimens were then fixed on glass slabs with Histoacryl topical tissue adhesive (B. Braun Corp., Melsungen, Germany), which was used according to manufacturer's instructions. The fixing luting agent was left to set for a period of 1 min before initiation of the measurements. For each specimen a time-period of 3 min was required for the preparation and testing procedures.

Specimens Topography

The specimens were first scanned in order their topography to be obtained. This can be achieved in two ways: (1) the contact mode and, (2) the tapping (semicontact) mode (Ethier and Simmons, 2008).

In the contact mode the probe exerts a constant force to the specimens, which has as a result the application of large lateral forces and therefore a possible deformation of the specimen (Ethier and Simmons, 2008). Thus, the tapping mode, in which the cantilever is either magnetically or acoustically driven, was selected. (Figure 2) During the scanning period the oscillating tip of the cantilever was moving in very close proximity to the surface of the specimen, touching it regularly.

The oscillations of the cantilever are due to repulsive and attracting forces, and they have been discussed previously in the literature (Goodman and Garcia, 1991; Garcia and San Paulo, 1999). The first ones are short range forces with an exponential decaying and can be considered as Pauli's exclusion principle interaction, electron-electron Coulomb interaction and hard sphere repulsion. The second ones are long range forces, including van der Waals interactions, electrostatic and chemical forces. For the interaction between the tip of the cantilever and

the specimen's surface, the van der Waals forces and van der Waals potential obey to the following (Hamaker, 1937):

$$F_{vdW} = - \left(\frac{AR}{6d^2} \right) \quad (1)$$

$$V_{vdW} = - \left(\frac{AR}{6d} \right) \quad (2)$$

Where, A is the Hamaker constant related to the material, R is the sphere radius and d is the separation between the tip and the half-space surface (Argento and French, 1996).

The scanning rate was set at $\sim 5,6 \mu\text{m/s}$ step 11 nm Hz, and the specimens' surface roughness was determined by the two following equations:

Mean absolute deviation surface roughness (R_a)

$$R_a = \frac{1}{N_x N_y} \sum_{i=1}^{N_x} \sum_{j=1}^{N_y} |Z(i, j) - Z_{mean}| \quad (3)$$

Where Z_{mean} represents the mean height, as this was calculated over the entire area of the biologic specimen, discretized in the grid of $Z(i, j)$, $i = 1, \dots, N_x$ and $j = 1, \dots, N_y$

The Root Mean Square (RMS) surface roughness

$$R_{RMS} = \sqrt{\frac{1}{N_x N_y} \sum_{i=1}^{N_x} \sum_{j=1}^{N_y} (Z(i, j) - Z_{mean})^2} \quad (4)$$

which represents the average deviation between the height and the mean surface.

Additionally, R_y (peak to valley) measurements were recorded. Two- and three-dimensional images of the specimens' topography were obtained (Figure 3).

Indentation Test

The mechanical properties of the specimens were then tested. The Si pyramidal tip traversed vertically toward the keratinized oral mucosa specimens and the deflection of the cantilever was measured. As the rigid tip moved toward the soft biologic

specimen the latter deflected around the probe. This problem of contact mechanics is based on the Hertz theory and the deflection of the cantilever arm is given by the following (Haga et al., 2002; Ethier and Simmons, 2008):

$$z - z_0 = \frac{F}{k_c} + \sqrt{\frac{\pi F(1 - \nu)}{2 E \tan \alpha}} \quad (5)$$

Where z is the vertical deflection, z_0 denotes the height of the probe where the force F applied to the biologic specimen becomes non-zero, k_c is the stiffness of the cantilever, E is the elastic modulus of the biologic material in N/m^{-2} , ν is the Poisson's ratio of the material (due to high water content Poisson's ratio for most biological specimens is considered to be 0.5), and α is the face angle for the silicon-nitride cantilever (Dimitriadis et al., 2002; Ethier and Simmons, 2008; **Figure 4**).

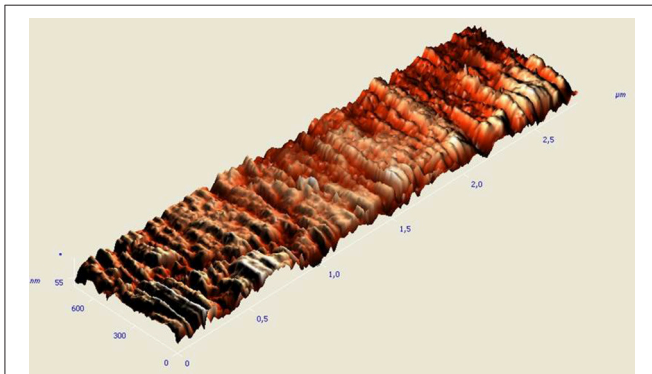


FIGURE 3 | Three-dimensional AFM image of keratinized oral mucosa.

The force applied by a four sided pyramidal tip is given by:

$$F = \frac{E(\delta)}{1 - \nu^2} \frac{\tan a}{\sqrt{2}} \delta^2 \quad (6)$$

$$\text{while, } a = \frac{\tan a}{\sqrt{2}} \delta \quad (7)$$

A vertical oscillating frequency of ~ 331 kHz was used and data were recorded at multiple sites of the tested specimens (Weisenhorn et al., 1992, 1993a,b; Stolz et al., 2004; Rahmat and Hubert, 2010; **Figure 5**). Each loading-unloading cycle lasted 0.3 s.

Force Calibration and Displacement Data

Identification of the first contact between the tip of the cantilever and the material tested presents a challenge in the indentation tests of soft biologic tissues, when using atomic force microscopy (Stolz et al., 2004; Herris et al., 2013). The abrupt change in the force-development curve, due to the generation of repulsive forces between the two interacting bodies, was taken as the initial contact point (z_0), and the corresponding force (F_0) at that point was zero.

The indentation depth was given by the following (Rahmat and Hubert, 2010; Herris et al., 2013):

$$h = (z - z_0) - (d - d_0) \quad (8)$$

where, z denotes the displacement of the cantilever base, d_0 represents the deflection of the cantilever at initial contact and d is the deflection of the cantilever. It should be pointed out that the cantilever's deflection was given by

$$d = d_0 + \left(\frac{F}{k}\right) \quad (9)$$

where, F represents the force and k denotes the stiffness of the cantilever.

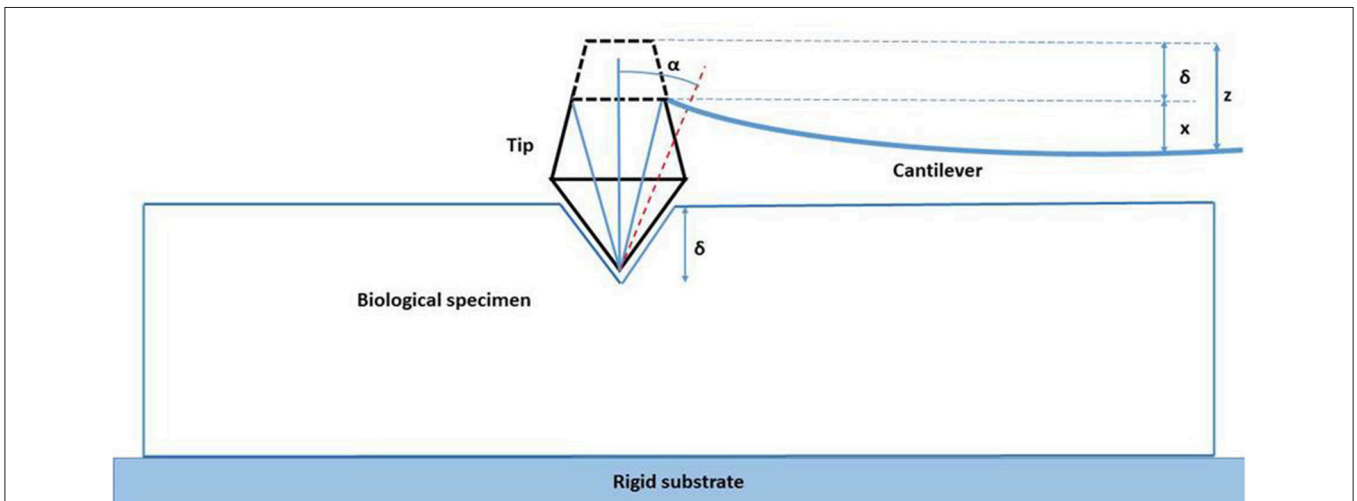


FIGURE 4 | Indentation of the human keratinized oral mucosa by the Si_3N_4 four-sided pyramid tip.

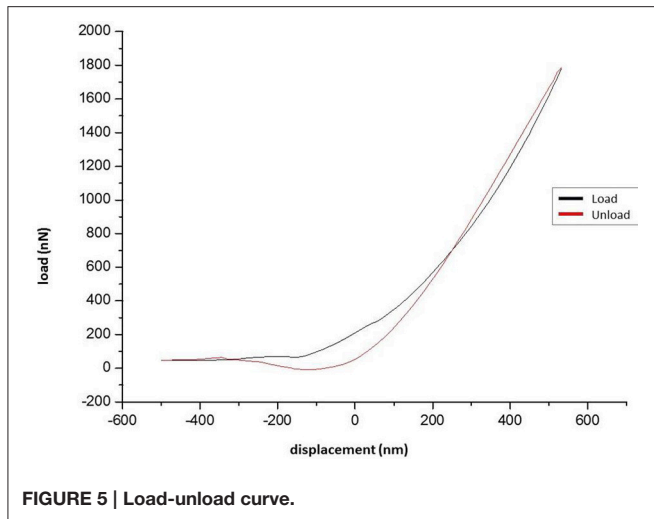


FIGURE 5 | Load-unload curve.

Room temperature ($21 \pm 1^\circ\text{C}$) and relative humidity ($50 \pm 10\%$) were recorded throughout the experiments.

RESULTS

The indentation tests were performed only on the coronal surface of the specimens. Indentation tests on sagittal planes were not performed due to their low clinical application.

Data from the indentation tests of the tested specimens was collected and force-displacement diagrams have been obtained (Figure 5). It should be mentioned that the negative values in the curve correspond to the initial phase of the testing procedure, when the tip lands on the surface of specimen.

Five loading-unloading cycles were registered. The simplest fitting approach was selected. That consisted of a visual inspection of the force-displacement curve and identification of the initial contact point (z_0, d_0), as already presented earlier (Lin et al., 2007). The area of the curve representing the noncontact region was ignored and for the contact region of the curve four mathematical models were tested using MATLAB (Mathworks Inc; Natick, MA, USA) to note which one approximates the force-displacement curve, as close as possible: a. spherical, b. conical, c. third order polynomial, d. Murphy (fourth order polynomial, non-linear Hertzian based), which is a fourth order polynomial model (Murphy et al., 2013; Table 1, Figure 6).

The goodness-of-fit measure presented in Table 1 is the normalized mean square error (NMSE), and was defined as follows:

$$NMSE = \frac{\sum_{i=1}^n (x_i - \hat{x}_i)^2}{\sum_{i=1}^n (x_i - \bar{x})^2} \quad (10)$$

where x_i is the i -th observation of variable X , \hat{x}_i is the corresponding estimated value by the fitted model, \bar{x} is the sample mean of the n observations of X .

The spherical and the conical models did not approximate the force-displacement curves. The model presented by Murphy et al.

TABLE 1 | Comparison of the numerical fit results including the goodness-of-fit statistic of the normalized mean square error, where the normalization is by the sample variance.

| Fit name | No.1 | No.2 | No.3 | No.4 | No.5 |
|--------------|----------|----------|----------|----------|----------|
| exp = 3/2 | 0.126403 | 0.009939 | 0.021102 | 0.003426 | 0.004355 |
| exp = 2 | 0.047443 | 0.085310 | 0.117485 | 0.060889 | 0.066963 |
| Murphy | 0.000380 | 0.002366 | 0.004634 | 0.002658 | 0.01629 |
| Polynomial 3 | 0.000396 | 0.000071 | 0.000142 | 0.000189 | 0.000023 |

(2013), with the form

$$F = \Gamma_1 \delta^4 + \Gamma_2 \delta^3 + \Gamma_3 \delta^2 \quad (11)$$

performed well for only one specimen.

The third order polynomial model of the form

$$f(\delta) = P_1 \delta^3 + P_2 \delta^2 + P_3 \delta + P_4 \quad (12)$$

approximated the curve very closely for all tested specimens.

Therefore, a proposition of a model which fits the experimental data better than the aforementioned models and the Hertz model (Herz, 1881), which is fully elastic, is attempted:

Murphy et al. (2013) have speculated that the Young's modulus of biological materials varies with displacement and is given by the following second order polynomial:

$$E(\delta) = k_1 \delta^2 + k_2 \delta + E_b \quad (13)$$

The authors hypothesized that the triad set k_1, k_2 , and E_b governs the modulus of elasticity of the material they tested. Specifically k_1 and k_2 represent the non-linear region, while E_b represents the contact stiffness, which is in the elastic region of the force-displacement curve.

The coefficients Γ_1, Γ_2 , and Γ_3 of their fourth order polynomial (11) are:

$$\Gamma_1 = \frac{2 k_1 (\tan a)}{\pi (1 - \nu^2)}, \quad (14)$$

$$\Gamma_2 = \frac{2 k_2 (\tan a)}{\pi (1 - \nu^2)}, \text{ and} \quad (15)$$

$$\Gamma_3 = \frac{2 E_b (\tan a)}{\pi (1 - \nu^2)} \quad (16)$$

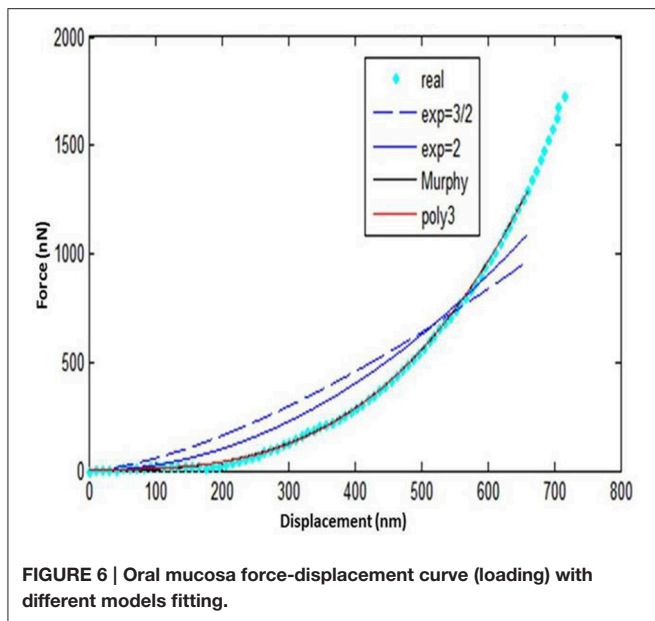
Accordingly, in the present study $E(\delta)$ is given by the following equation:

$$E(\delta) = k_1 \delta + k_2 + E_b \quad (17)$$

where k_1, k_2 , and E_b describe the oral mucosa's and mucoperiosteum's properties as a triad set, and

$$E_b = \frac{k_3}{\delta} \quad (18)$$

E_b represents the mucoperiosteum's contact stiffness and δ is the indentation depth.



A similar approach has been adopted by Murphy et al. (2013). Other researchers have come independently to the same conclusion (Herris et al., 2013).

The constant term P_4 of (12) is omitted, as when $F = 0$, $\delta = 0$. Then the general polynomial model (12) becomes:

$$F = P_1\delta^3 + P_2\delta^2 + P_3\delta \quad (19)$$

Therefore, by substituting $E(\delta)$ from (17) and (18) to (6), the latter becomes:

$$F = \frac{k_1 \tan a}{(1 - \nu^2)\sqrt{2}} \delta^3 + \frac{k_2 \tan a}{(1 - \nu^2)\sqrt{2}} \delta^2 + \frac{k_3 \tan a}{(1 - \nu^2)\sqrt{2}} \delta \quad (20)$$

where F is the applied force, δ is the indentation depth, α is the face angle for the silicon-nitride cantilever, ν is the Poisson's ratio of the mucosa, and k_1 , k_2 , and k_3 are the moduli of elasticity for the stratified squamous epithelium, lamina propria and mucoperiosteum respectively.

DISCUSSION

In the present *ex vivo* study AFM was used to test the mechanical properties of human keratinized oral mucosa. The specimens were harvested from the edentulous areas which support the maxillary complete denture (Hobkirk and Zarb, 2013). The force-development curves were analyzed and a third order polynomial model different than the classic elastic Hertz model (Herz, 1881) was developed in order to describe its biomechanical response.

In the past 25 years AFM has been used to study the mechanical properties of materials. This concept has also been used in the early 90's for "force-displacement" data collection from biological materials, including tendons, ligaments, muscle tissues and menisci (Burnham and Colton, 1989; Radmacher et al., 1992; Tao et al., 1992; Weiss et al., 2002; Sweigart et al.,

2004; Yin and Elliot, 2004; Van Loocke et al., 2006, 2008; Villegas et al., 2007; Cheng and Gan, 2008; Ciarletta et al., 2008). A nano-indenter could have been used in this study, as well. However, nano-indenters have a resolution of approximately 100 nN, while the forces applied by the AFM can range from pico-Newtons to several hundreds of micro-Newtons by changing the stiffness of the cantilever. Thus, the sensitivity and the versatility of the AFM makes it an ideal tool for mechanical properties testing of biological materials (Stolz et al., 2009; Notbohm et al., 2012). Additionally, use of the tapping mode of the AFM prevents the distortion of the biologic specimen, as it is presented later in the discussion. In most of the published research, standard manufacturers' cantilevers and pyramidal tips have been employed, while modifications with attachment of silica microspheres have also been reported (Mahaffy et al., 2000; Dimitriadis et al., 2002). The solution for the microsphere tips is supplied by the original Hertz model which deals with the shallow contact between two spherical bodies (Herz, 1881). The original Hertzian theory has been used by many researchers who studied contact deformation and many modifications have been made in order to account for large deformations (Gao and Gao, 2000), viscoelasticity (Gillies et al., 2002; Yang et al., 2004; Attard, 2007; Chen et al., 2013), anisotropy (Batra and Jiang, 2008), multi-layered structures (Ai et al., 2002), and adhesive interactions (Cao et al., 2005; Yang, 2006; Ebenstein, 2011; Chen et al., 2013; Kohn and Ebenstein, 2013). In the present study a sharp pyramidal tip was employed. It should be mentioned that the Bilodeau solution applies for this case (Bilodeau, 1992).

The model developed in the present study is probably valid only when the forces are applied to the coronal part of the oral keratinized mucosa, as it has been proven that tissues are both inhomogeneous and anisotropic. Biological specimens' anisotropic properties have been demonstrated with nonlinear laser scanning microscopy, which has been used for elastin and collagen distribution—within the specimens—imaging (Herris et al., 2013). Additionally their mechanical properties are site and direction-specific dependent (Stolz et al., 2004). It has been shown in the past that the indentation elastic moduli of biological specimens differ depending on the depth, increasing from the superficial to deep layers (Herris et al., 2013). Furthermore, it has been demonstrated that both the Young's modulus and Poisson's ratio change during different development stages of the cell (Zhang et al., 2009). Three different moduli of elasticity were incorporated to the model developed in this study, with k_1 being the modulus of elasticity of stratified squamous epithelium, k_2 of lamina propria and k_3 of mucoperiosteum. This is in accordance with the present experimental results and previous research findings, which have demonstrated that the elastic moduli increase from the superficial to the deep layer (Herris et al., 2013; Murphy et al., 2013). Furthermore, the cells and the extracellular matrix present different elastic modulus and may contribute to the observed inhomogeneity (Trickey et al., 2006; Han et al., 2011). Third-degree polynomial models have also proven to be valid for mechanical forces acting on cell biomembranes, as well as in other anatomical structures as the descending aorta (Stefanadis et al., 2000; Zhang et al., 2009). The third degree polynomial model without a constant term which

was tested in the present study not only approximated better the force-displacement curve of the keratinized oral mucosa, but it also provided a simpler model than the fourth order polynomial presented by Murphy et al. (2013). It should be mentioned however that different biological tissues have been examined in these two studies.

As already mentioned, before testing the specimens were kept in a buffered 10% formalin solution until testing, which occurred within an hour. The 10% formalin solution is actually a 4% formaldehyde, which is by definition 1.3 molar. A totally unbuffered formaldehyde solution exerts an osmotic pressure of about 1300 mO. Isotonic salt solutions present osmolarities of 250–350 mO. Therefore, it is expected that formalin diffuses into tissues faster. Formaldehyde has a molecular weight of 30 and it is expected to penetrate the tissues fast. Nevertheless, fixation actually takes a relatively long time. It has been estimated that a time period of 6–16 h, depending on the specimen, is needed. Furthermore, since all specimens received the same treatment simultaneously it can be assumed that formalin penetration was uniform in all specimens. Macroscopically, no swelling was noticed within the 1-h period between specimen harvesting and testing (Bono et al., 2001; Thavarajah et al., 2012).

The human oral keratinized tissue tested in the present study was bonded with cyanoacrylate cement to a glass slab, since there is scientific evidence that force-displacement results depend strongly on whether or not the specimens are attached to the substrate (Yang, 1998). A glass substrate was used as its modulus of elasticity is 50 GPa, which is much higher than that of biologic specimens, while the modulus of elasticity of the pyramidal tip employed was 150 GPa (Grafström et al., 1993; Weisenhorn et al., 1993a). Therefore, the deformation of both the tip and the substrate can be considered as negligible.

The loading-unloading curves of the specimens tested did not coincide, suggesting a viscoelastic behavior (Lakes, 1999). Furthermore, the hysteresis of the loading-unloading curves, indicates dissipation of energy. During loading, the area beneath represents the energy stored, while during unloading, this area represents the energy recovered. Quantification of the hysteresis can be performed by introduction of the plasticity index η . In experiments involving solid objects this parameter characterizes the elastic/plastic behavior of the material, when external forces are applied. The value of plasticity index can range between 0, indicating a fully elastic material, and 1, when the material displays a fully plastic behavior (Briscoe et al., 1998; Klymenko et al., 2009).

The tapping mode was selected for the present study, as it presents more advantages than the contact and the non-contact imaging methods. The tapping mode eliminates the lateral, frictional forces transmitted from the tip of the cantilever to the specimen's surface. In this mode the probe oscillates with sufficient amplitude to prevent it being trapped by adhesive meniscus forces from the contaminant layer (e.g., water), and it makes intermittent contact with the surface of the specimen (Manning et al., 2003; Rogers et al., 2004). As a result, tissue damage is minimal, if any, and recovery is guaranteed. The oscillation frequency usually ranges between 50,000 and 500,000 cycles per second. An oscillation frequency of 311,000 cycles was

used in the present study. With this frequency the tip-specimen adhesion forces are overcome and only vertical forces are applied. The high frequency oscillations of the tip may be regarded as a disadvantage of the method, as they are not comparable to the human chewing frequency. It should be mentioned however that, neither the forces applied by the tip to the specimen are comparable to mastication forces. Atomic force microscopy, like all laboratory techniques, has some limitations.

It should be pointed out however that, in studies like the present one, a fundamental assumption is made: the mechanical response of biological materials relies on contribution of different structures which act in sequence. In this way interpretation of the mechanical properties of materials which present a hierarchy can be made (Bonilla et al., 2015).

Development of a model describing the behavior of oral mucosa under mechanical forces is instrumental for the knowledge of its mechanical properties, such as the Young's modulus, and an understanding of how masticatory function is affected by mechanical interactions. Moreover, this modeling assists in fabricating biomaterials (e.g., tissue conditioners) which will act in a similar way with, or in a complimentary way to the oral keratinized mucosa.

It should be mentioned that *ex-vivo* studies performed with AFM present certain drawbacks, including the identification of the most appropriate area for force application, the high frequency oscillation of the cantilever, the possible minor dehydration of the tissue, the molecular roughness of the pyramidal tip and the uncertainty of the first contact between the tip and the biological specimen. These have also been acknowledged by other authors and possibly affect measurement's accuracy (Vinckier and Semenza, 1998).

Further studies are needed to determine the contribution of each layer, as well as, that of the cells and the extracellular matrix in the biomechanical behavior of the oral mucosa.

CONCLUSION

Within the limitations of the present study, the following conclusions can be made regarding the force-displacement data of the human oral keratinized mucosa:

- (1) The third order polynomial model examined in the present study showed a very good accuracy.
- (2) The Murphy model (fourth order) performed well for only one specimen.
- (3) The spherical and the conical models did not approximate the force-displacement curves.
- (4) A mathematical model for the analysis of the biomechanical response of human keratinized oral mucosa was developed.

AUTHOR NOTE

The results of this paper were presented at the IADR General Session, March 20–23, 2013, Seattle, WA, USA, and at the European Society of Biomechanics, August 25–28, 2013, Patras, Greece.

AUTHOR CONTRIBUTIONS

All authors (AT, PK, MS, SK, DK, SL, ON, AP, and KM) have made substantial contributions to the conception and/or design of the work; or the acquisition, analysis, or interpretation of data for the work; and greatly assisted

in drafting the work or revising it critically for important intellectual content; and they approved the submitted version; and agreed to be accountable for all aspects of the work in ensuring that questions related to the accuracy or integrity of any part of the work are appropriately investigated and resolved.

REFERENCES

- Ai, Z. Y., Yue, Z. Q., Tham, L. G., and Yang, M. (2002). Extended Sneddon and Muki solutions for multilayered elastic materials. *Int. J. Eng. Sci.* 40, 1453–1483. doi: 10.1016/S0020-7225(02)00022-8
- Argento, C., and French, R. H. (1996). Parametric tip model and force-distance relation for Hamaker constant determination from atomic force microscopy. *J. Appl. Phys.* 80, 6081–6090. doi: 10.1063/1.363680
- Atkinson, H. F., and Ralph, W. J. (1977). *In vitro* strength of the human periodontal ligament. *J. Dent. Res.* 56, 48–52. doi: 10.1177/00220345770560011001
- Attard, P. (2007). Measurement and interpretation of elastic and viscoelastic properties with the atomic force microscope. *J. Phys. Condens. Matter.* 19, 47320161. doi: 10.1088/0953-8984/19/47/473201
- Batra, R. C., and Jiang, W. (2008). Analytical solution of the contact problem of a rigid indenter and an anisotropic linear elastic layer. *Int. J. Solids Struct.* 45, 5814–5830. doi: 10.1016/j.ijsolstr.2008.06.016
- Bergomi, M., Cugnomi, J., Botsis, J., Belser, U. C., and Wiskott, H. W. (2010). The role of the fluid phase in the viscous response of bovine periodontal ligament. *J. Biomech.* 43, 1146–1152. doi: 10.1016/j.jbiomech.2009.12.020
- Bergomi, M., Cugnomi, J., Galli, M., Botsis, J., Belser, U. C., and Wiskott, H. W. (2011). Hydro-mechanical coupling in the periodontal ligament: a porohyperelastic finite element model. *J. Biomech.* 44, 34–38. doi: 10.1016/j.jbiomech.2010.08.019
- Bien, S. M. (1966). Hydrodynamic damping of tooth movement. *J. Dent. Res.* 45, 907–914. doi: 10.1177/00220345660450036701
- Bilodeau, G. (1992). Regular pyramid punch problem. *J. Appl. Mech.* 59, 519–523. doi: 10.1115/1.2893754
- Blaushild, N., Mihaeli, Y., and Steigman, S. (1992). Histomorphometric study of the periodontal vasculature of the rat incisor. *J. Dent. Res.* 71, 1908–1912. doi: 10.1177/00220345920710121001
- Bonilla, M. R., Stokes, J. R., Gidley, M. J., and Yakubov, G. E. (2015). Interpreting atomic force microscopy nanoindentation of hierarchical biological materials using multi-regime analysis. *Soft Matter.* 11, 1281–1292. doi: 10.1039/C4SM02440K
- Bono, C., Renard, R., Sabatino, C., Levine, R., and Tornetta, P. (2001). “The effects of varied concentrations of formalin on the tensile strength of cortical bone: should embalmed bone ever be used for biomechanical testing,” in *Orthopedics Research Society, 47th Annual Meeting February* (San Francisco, CA).
- Bourke, K. A., Haasse, H., Li, H., Daley, T., and Bartold, P. M. (2000). Distribution and synthesis of elastin in porcine gingiva and alveolar mucosa. *J. Periodont. Res.* 35, 361–368. doi: 10.1034/j.1600-0765.2000.035006361.x
- Briscoe, B. J., Fiori, L., and Pelillo, E. (1998). Nano-indentation of polymeric surfaces. *J. Phys. D Appl. Phys.* 31, 2395–2405. doi: 10.1088/0022-3727/31/19/006
- Burnham, N. A., and Colton, R. J. (1989). Measuring the nanomechanical properties and surface forces of materials using the AFM. *J. Vac. Sci. Technol.* 7, 2906–2913. doi: 10.1116/1.576168
- Cao, Y. F., Yang, D. H., and Soboyejoy, W. (2005). Nanoindentation method for determining the initial contact and adhesion characteristics of soft polydimethylsiloxane. *J. Mater. Res.* 20, 2004–2011. doi: 10.1557/JMR.2005.0256
- Caputo, A. A., and Standlee, J. P. (1987). *Biomechanics in Clinical Dentistry*. Chicago, IL: Quintessence.
- Carranza, F. A. (1990). *Glickman's Clinical Periodontology*. Philadelphia, PA: W. B. Saunders.
- Chen, J., Ahmad, R., Li, W., Swain, M., and Li, Q. (2015). Biomechanics of oral mucosa. *J. R. Interface* 12:20150325. doi: 10.1098/rsif.2015.0325
- Chen, Z., Diebels, S., Peter, N. J., and Schneider, A. S. (2013). Identification of finite viscoelasticity and adhesion effects in nanoindentation of a soft polymer by inverse method. *Comput. Mater. Sci.* 72, 127–139. doi: 10.1016/j.commatsci.2013.01.040
- Cheng, T., and Gan, R. Z. (2008). Mechanical properties of anterior malleolar ligament from experimental measurement and material modelling analysis. *Biomech. Model. Mechanobiol.* 7, 387–394. doi: 10.1007/s10237-007-0094-x
- Ciarletta, P., Dario, P., and Micera, S. (2008). Pseudo-hyperelastic model of tendon hysteresis from adaptive recruitment of collagen type I fibrils. *Biomaterials* 29, 764–770. doi: 10.1016/j.biomaterials.2007.10.020
- Clausen, H., Vedtofte, P., Moe, D., and Dabelsteen, E. (1983). Keratin pattern in human and buccal and hard palate mucosa. *Scand. J. Dent. Res.* 91, 411–413. doi: 10.1111/j.1600-0722.1983.tb00838.x
- Dahlhöf, G., Mondèer, T., Reinholt, F. P., Wilkström, B., and Hjerpe, A. (1986). Proteoglycans and glycosaminoglycans in phenytoin -induced gingival overgrowth. *J. Periodont. Res.* 21, 13–21. doi: 10.1111/j.1600-0765.1986.tb01432.x
- Daly, C. H., Nicholls, J. I., Kydd, W. L., and Nansen, P. D. (1974). The response of the human periodontal ligament to torsional loading-I. Experimental methods. *J. Biomech.* 7, 517–522. doi: 10.1016/0021-9290(74)90086-4
- Dimitriadis, E. K., Horkay, F., Maresca, J., Kachar, B., and Chadwick, R. S. (2002). Determination of elastic moduli of thin layers of soft material using the atomic force microscope. *Biophys. J.* 82, 2798–2810. doi: 10.1016/S0006-3495(02)75620-8
- Dorow, C., Kristin, N., and Sander, F. G. (2003). Determination of the mechanical properties of the periodontal ligament in a uniaxial tensional experiment. *J. Orofac. Orthop.* 64, 100–107. doi: 10.1007/s00056-003-0225-7
- Ebenstein, D. M. (2011). Nano-JKR force curve method overcomes challenges of surface detection and adhesion for nanoindentation of a compliant polymer in air and water. *J. Mater. Res.* 26, 1026–1035. doi: 10.1557/jmr.2011.42
- Embery, G., Waddington, R., and Hall, R. (1995). “The ground substance of the periodontal ligament,” in *The Periodontal Ligament in Health and Disease*, eds B. K. B. Berkovitz, B. J. Moxham, and H. N. Newman (London: Mosby-Wolfe), 83–106.
- Ethier, C. R., and Simmons, C. A. (2008). *Introductory Biomechanics. From Cells to Organisms*. Cambridge: University Press.
- Fung, Y. C. (1973). Biorheology of soft tissues. *Biorheology* 10, 139–155.
- Gao, Y. C., and Gao, T. J. (2000). Large deformation contact of a rubber notch with a rigid wedge. *Int. J. Solids Struct.* 37, 4319–4334. doi: 10.1016/S0020-7683(99)00191-2
- García, R., and San Paulo, A. (1999). Attractive and repulsive tip-sample interaction regimes in tapping-mode atomic force microscopy. *Phys. Rev. B.* 60, 4961–4967. doi: 10.1103/PhysRevB.60.4961
- Gillies, G., Prestidge, C. A., and Attard, P. (2002). An AFM study of the deformation and nanorheology of cross-linked PDMS droplets. *Langmuir* 18, 1674–1679. doi: 10.1021/la011461g
- Goktas, S., Dmytryk, J. J., and McFetridge, P. S. (2011). Biomechanical behavior of oral soft tissues. *J. Periodontol.* 82, 1178–1186. doi: 10.1902/jop.2011.100573
- Goodman, F. O., and Garcia, N. (1991). Roles of the attractive and repulsive forces in atomic-force microscopy. *Phys. Rev. B.* 43, 4728–4731. doi: 10.1103/PhysRevB.43.4728
- Grafström, S., Neitzert, M., Hagen, T., Ackermann, J., Neuman, R., Ptobst, O., et al. (1993). The role of topography and friction for the image contrast in lateral force microscopy. *Nanotechnology* 4, 143–151. doi: 10.1088/0957-4484/4/3/003
- Haga, H., Sasaki, S., Kawabata, K., Ito, E., Ushiki, T., and Sambongi, T. (2002). Elasticity mapping of living fibroblasts by AFM and immunofluorescence

- observation of the cytoskeleton. *Ultramicroscopy* 82, 253–258. doi: 10.1016/S0304-3991(99)00157-6
- Hamaker, H. C. (1937). The London-van der Waals attraction between spherical particles. *Physica* 4, 1058–1072. doi: 10.1016/S0031-8914(37)80203-7
- Han, L., Grodzinsky, A. J., and Ortiz, C. (2011). Nanomechanics of the cartilage extracellular matrix. *Annu. Rev. Mater. Res.* 41, 133–168. doi: 10.1146/annurev-matsci-062910-100431
- Herris, H. K., Miri, A. K., Tripathy, U., Barthelat, F., and Mongeau, L. (2013). Indentation of poroviscoelastic vocal fold tissue using an atomic force microscope. *J. Mech. Behav. Biomed. Mater.* 28, 383–392. doi: 10.1016/j.jmbm.2013.05.026
- Herz, H. (1881). Über die berührung fester elastischer körper. *J. die reine und Angewandte Mathematik* 92, 156–171.
- Hobkirk, J. A., and Zarb, G. (2013). “The edentulous state,” in *Prosthodontic Treatment for Edentulous Patients. Complete Dentures and Implant-Supported Prostheses, 13th Edn.*, eds G. Zarb, J. A. Hobkirk, S. E. Eckert, and R. F. Jacob (St. Louis, MO: Elsevier Mosby), 1–27.
- Hong, G., Maeda, T., Murata, H., and Sasaki, K. (2012). The dynamic viscoelasticity and plasticizer leachability of tissue conditioners. *Gerodontology* 29, 284–291. doi: 10.1111/j.1741-2358.2012.00639.x
- Ioi, H., Morishita, T., Nakata, S., Nakashima, A., and Nanda, R. S. (2002a). Evaluation of physiological tooth movements within clinically normal periodontal tissues by means of periodontal pulsation measurements. *J. Periodont. Res.* 37, 110–117. doi: 10.1034/j.1600-0765.2001.00665.x
- Ioi, H., Nakata, S., Nakashima, A., Counts, A. L., and Nanda, R. S. (2002b). Changes in tooth position in humans in relation to arterial blood pressure. *Arch. Oral Biol.* 47, 219–226. doi: 10.1016/S0003-9969(01)00110-8
- Johnson, R. B., and Pylpyas, S. P. (1992). A re-evaluation of the distribution of the elastic meshwork within the periodontal ligament of the mouse. *J. Periodont. Res.* 27, 239–249. doi: 10.1111/j.1600-0765.1992.tb01674.x
- Jonas, I. E., and Riede, U. N. (1980). Reaction of oxytalan fibers in human periodontium to mechanical stress. A combined histochemical and morphometric analysis. *J. Histochem. Cytochem.* 28, 211–216. doi: 10.1177/28.3.7354216
- Kardos, T. B., and Simpson, L. O. (1979). A theoretical consideration of the periodontal membrane as a collagenous thixotropic system and its relationship to tooth eruption. *J. Periodont. Res.* 14, 444–451. doi: 10.1111/j.1600-0765.1979.tb00243.x
- Kardos, T. B., and Simpson, L. O. (1980). A new periodontal membrane biology based on thixotropic concepts. *Am. J. Orthod.* 77, 508–515. doi: 10.1016/0002-9416(80)90130-X
- Keilig, L., Stark, H., Bayer, S., Utz, K. H., Strazza, M., Grünner, M., et al. (2009). Numerical investigation of the mechanical loading of supporting soft tissue for partial dentures. *Int. J. Prosthodont.* 22, 201–203.
- Klymenko, O., Wiltowska-Zuber, J., Lekka, M., and Kwiatek, W. M. (2009). Energy dissipation in the AFM elasticity measurements. *Acta Phys. Pol. A.* 115, 548–551. doi: 10.12693/APhysPolA.115.548
- Kohn, J. C., and Ebenstein, D. M. (2013). Eliminating adhesion errors in nanoindentation of compliant polymers and hydrogels. *J. Mech. Behav. Biomed. Mater.* 20, 316–326. doi: 10.1016/j.jmbm.2013.02.002
- Komatsu, K., and Viidik, A. (1966). Changes in the fibre arrangement of the rat incisor periodontal ligament in relation to various loading levels *in vitro*. *Arch. Oral Biol.* 41, 147–159. doi: 10.1016/0003-9969(95)00114-X
- Kristiansen, A. B., and Heyreaas, K. J. (1989). Micropuncture measurements of interstitial fluid pressure in the rat periodontal ligament. *Proc. Finn. Dent. Soc.* 85, 295–300.
- Kurashima, K. (1965). Viscoelastic properties of periodontal tissue. *Bull. Tokyo Med. Dent. Univ.* 36, 148–153.
- Lakes, R. S. (1999). *Viscoelastic Solids*. Boca Raton, FL: CRC Press.
- Lin, D. C., Dimitriadis, E. K., and Horkay, F. (2007). Robust strategies for automated AFM force curve analysis-I. Non-adhesive indentation of soft inhomogenous materials. *J. Biomech. Eng.* 129, 430–440. doi: 10.1115/1.2720924
- Lindhe, J., Karring, T., and Lang, N. P. (2003). *Clinical Periodontology and Implant Dentistry*. Copenhagen: Blackwell Munksgaard.
- Mahaffy, R. E., Shih, C. K., MacKintosh, F. C., and Käs, J. (2000). Scanning probe-based frequency-dependent microrheology of polymer gels and biological cells. *Phys. Rev. Lett.* 85, 880–883. doi: 10.1103/PhysRevLett.85.880
- Manning, L., Rogers, B., Jones, M., Adams, J. D., Fuste, J. L., and Minne, S. C. (2003). Self-oscillating tapping mode atomic force microscopy. *Rev. Sci. Instrum.* 74, 4220–4222. doi: 10.1063/1.1602935
- Meyer, J., Squier, C. A., and Gerson, S. J. (1984). *The Structure and Function of Oral Mucosa*. Oxford: Pergamon Press.
- Michalakos, K. X., Calvani, P., and Hirayama, H. (2012). Biomechanical considerations on tooth-implant supported fixed partial dentures. *J. Dent. Biomech.* 3:1758736012462025 doi: 10.1177/1758736012462025
- Mühlemann, H. R. (1951). Periodontometry, a method for measuring tooth mobility. *Oral Surg. Oral Med. Oral Path* 4, 1220–1233. doi: 10.1016/0030-4220(51)90080-1
- Murphy, M. F., Lilley, F., Lalor, M. J., Crosby, S. R., Madden, G., Johnston, G., et al (2013). Evaluation of a nonlinear Hertzian-based model reveals prostate cancer cells respond differently to force than normal prostate cells. *Microsc. Res. Tech.* 76, 36–41. doi: 10.1002/jemt.22132
- Nanci, A. (2013). *Ten Cate's Oral Histology*. St. Louis, MO: Elsevier Mosby.
- Natali, A. N., Pavan, P. G., Carniel, E. L., and Dorow, C. (2003). A transversally isotropic elasto-damage constitutive model for the periodontal ligament. *Comput. Methods Biomech. Biomed. Engin.* 6, 329–336. doi: 10.1080/10255840310001639840
- Natali, A. N., Pavan, P. G., Carniel, E. L., and Dorow, C. (2004). Visco-elastic response of the periodontal ligament: an experimental-numerical analysis. *Connect. Tissue Res.* 45, 222–230. doi: 10.1080/03008200490885742
- Newcomb, G. M. (1981). An ultrastructural study of epithelial specialization at the porcine mucogingival junction. *J. Periodont. Res.* 16, 51–65. doi: 10.1111/j.1600-0765.1981.tb00949.x
- Notbohm, J., Poon, B., and Ravichandran, G. (2012). Analysis of nanoindentation of soft materials with an atomic force microscope. *J. Mater. Res.* 27, 229–237. doi: 10.1557/jmr.2011.252
- Picton, D. C. (1965). On the part played by the socket on tooth support. *Arch. Oral Biol.* 6, 945–955. doi: 10.1016/0003-9969(65)90088-9
- Picton, D. C. (1969). “The effect of external forces on the periodontium,” in *Biology of the Periodontium*, eds A. H. Melcher and W. H. Bowen (New York, NY: Academic Press), 363–419.
- Radmacher, M., Tillman, R. W., Fritz, M., and Gaub, H. E. (1992). From molecules to cells: imaging soft samples with the atomic force microscope. *Science* 257, 1900–1905. doi: 10.1126/science.1411505
- Rahmat, B., and Hubert, P. (2010). Interaction stress measurement using atomic force microscopy: a stepwise discretization method. *J. Phys. Chem. C.* 114, 15029–15035. doi: 10.1021/jp104993f
- Rogers, B., Manning, L., Sulchek, T., and Adams, J. D. (2004). Improving tapping mode atomic force microscopy with piezoelectric cantilevers. *Ultramicroscopy* 100, 267–276. doi: 10.1016/j.ultramic.2004.01.016
- Sader, J. E., Chon, J. W. M., and Mulvaney, P. (1999). Calibration of rectangular atomic force microscope cantilevers. *Rev. Sci. Instrum.* 70, 3967–3969. doi: 10.1063/1.1150021
- Saitoh, S., Sasaki, K., Nezu, T., and Taira, M. (2010). Viscoelastic behavior of commercially available tissue conditioners under compression. *Dent. Mater. J.* 29, 461–468. doi: 10.4012/dmj.2009-130
- Sims, M. (1995). “The morphology of the vasculature of the periodontal ligament,” in *The Periodontal Ligament in Health and Disease*, eds B. K. B. Berkovitz, B. J. Moxham, and H. N. Newman (London: Mosby-Wolfe), 107–20.
- Slavkin, H. C., and Bavetta, L. A. (1972). *Developmental Aspects of Oral Biology*. New York, NY: Academic Press.
- Sloan, P., and Carter, D. H. (1995). “Structural organization of the fibres of the periodontal ligament,” in *The Periodontal Ligament in Health and Disease*, eds B. K. B. Berkovitz, B. J. Moxham, and H. N. Newman (London: Mosby-Wolfe).
- Stefanadis, C., Dernelis, J., Tsiamis, E., Diamantopoulos, L., Michaelides, A., and Toutouzas, P. (2000). Assessment of aortic line of elasticity using polynomial regression analysis. *Circulation* 101, 1819–1825. doi: 10.1161/01.CIR.101.15.1819
- Stolz, M., Gottardi, R., Raitteri, R., Miot, S., Martin, I., Imer, R., et al. (2009). Early detection of aging cartilage and osteoarthritis in mice and patient samples using atomic force microscopy. *Nat. Nanotechnol.* 4, 186–192. doi: 10.1038/nnano.2008.410

- Stolz, M., Raiteri, R., Daniels, A. U., VanLandingham, M. R., Baschong, W., and Aebi, U. (2004). Dynamic elastic modulus of porcine articular cartilage determined at two different levels of tissue organization by indentation-type atomic force microscopy. *Biophys. J.* 86, 3269–3283. doi: 10.1016/S0006-3495(04)74375-1
- Sweigart, M. A., Zhu, C. F., Burt, D. M., DeHoll, P. D., Agrawal, C. M., Clanton, T. O., et al. (2004). Intraspecies and interspecies comparison of the compressive properties of the medial meniscus. *Ann. Biomed. Eng.* 32, 1569–1579. doi: 10.1114/B:ABME.0000049040.70767.5c
- Tao, N. J., Lindsay, S. M., and Lees, S. (1992). Measuring the microelastic properties of biological materials. *Biophys. J.* 63, 1165–1169. doi: 10.1016/S0006-3495(92)81692-2
- Thavarajah, R., Mudimbaimannar, V. K., Elizabeth, J., Rao, U. K., and Ranganatham, K. (2012). Chemical and physical basics of routine formaldehyde fixation. *J. Oral Maxillofac. Pathol.* 16, 400–405. doi: 10.4103/0973-029X.102496
- Trickey, W. R., Baaijens, F. P., Laursen, T. A., Alexopoulos, L. G., and Guilak, F. (2006). Determination of the Poisson's ratio of the cell: recovery properties of chondrocytes after release from complete micropipette aspiration. *J. Biomech.* 39, 78–87. doi: 10.1016/j.jbiomech.2004.11.006
- Van Loocke, M., Lyons, C. G., and Simms, C. K. (2006). A validated model of passive muscle in compression. *J. Biomech.* 39, 2999–3009. doi: 10.1016/j.jbiomech.2005.10.016
- Van Loocke, M., Lyons, C. G., and Simms, C. K. (2008). Viscoelastic properties of skeletal muscle in compression: stress-relaxation behavior and constitutive modelling. *J. Biomech.* 41, 1555–1566. doi: 10.1016/j.jbiomech.2008.02.007
- Villegas, D. F., Maes, J. A., Magee, S. D., and Donahue, T. L. (2007). Failure properties and strain distribution analysis of meniscal attachments. *J. Biomech.* 40, 2655–2662. doi: 10.1016/j.jbiomech.2007.01.015
- Vinckier, A., and Semenza, G. (1998). Measuring elasticity of biological materials by atomic force microscopy. *FEBS Lett.* 430, 12–16. doi: 10.1016/S0014-5793(98)00592-4
- Weisenhorn, A. L., Kasas, S., Solletti, J. M., Khorsandi, M., Gotzos, V., Romer, D. U., et al. (1993a). Deformation observed on soft surfaces with an AFM. *Proc. SPIE* 1855 26–34. doi: 10.1117/12.146382
- Weisenhorn, A. L., Khorsandi, M., Kasas, S., Gotzos, V., and Butt, H. J. (1993b). Deformation and height anomaly of soft surfaces studied with an AFM. *Nanotechnology* 4, 106–113. doi: 10.1088/0957-4484/4/2/006
- Weisenhorn, A. L., Maivald, P., Butt, H. J., and Hansma, P. K. (1992). Measuring adhesion, attraction, and repulsion between surfaces in liquids with an atomic-force microscope. *Phys. Rev. B. Condensed. Matt.* 45, 11226–11232. doi: 10.1103/PhysRevB.45.11226
- Weiss, J. A., Gardiner, J. C., and Bonifasi-Lista, C. (2002). Ligament material behavior is nonlinear, viscoelastic and rate-independent under shear loading. *J. Biomech.* 35, 943–950. doi: 10.1016/S0021-9290(02)00041-6
- Wills, D. J., and Picton, D. C. (1978). Changes in the mobility and resting position of incisor teeth in macaque monkeys. *Arch. Oral. Biol.* 23, 225–229. doi: 10.1016/0003-9969(78)90221-2
- Wills, D. J., Picton, D. C., and Davies, W. I. R. (1976). A study of the fluid systems of the periodontium in macaque monkeys. *Arch. Oral. Biol.* 21, 175–185. doi: 10.1016/0003-9969(76)90127-8
- Yang, F. (1998). Indentation of an incompressible elastic film. *Mech. Mater.* 30, 275–286. doi: 10.1016/S0167-6636(98)00035-0
- Yang, F. (2006). Effect of adhesion energy on the contact stiffness in nanoindentation. *J. Mater. Res.* 21, 2683–2688. doi: 10.1557/jmr.2006.0331
- Yang, S., Zhang, Y. W., and Zeng, K. Y. (2004). Analysis of nanoindentation creep for polymeric materials. *J. Appl. Phys.* 95, 3655–3666. doi: 10.1063/1.1651341
- Yin, L., and Elliot, D. M. (2004). A biphasic and transversely isotropic mechanical model for tendon: application to mouse tail fascicles in uniaxial tension. *J. Biomech.* 37, 907–916. doi: 10.1016/j.jbiomech.2003.10.007
- Zhang, Y. L., Han, M. L., Vidyalakshmi, J., Shee, C. Y., and Ang, W. T. (2009). Automatic control of mechanical forces acting on cell biomembranes using a vision-guided microrobotic system in computer microscopy. *J. Microsc.* 236, 70–78. doi: 10.1111/j.1365-2818.2009.03209.x

Conflict of Interest Statement: The authors declare that the research was conducted in the absence of any commercial or financial relationships that could be construed as a potential conflict of interest.

Copyright © 2016 Tsaira, Karagiannidis, Sidira, Kassavetis, Kugiumtzis, Logothetidis, Naka, Pissiotis and Michalakis. This is an open-access article distributed under the terms of the Creative Commons Attribution License (CC BY). The use, distribution or reproduction in other forums is permitted, provided the original author(s) or licensor are credited and that the original publication in this journal is cited, in accordance with accepted academic practice. No use, distribution or reproduction is permitted which does not comply with these terms.